

Microscopic Motion of Particles Flowing through a Porous Medium

Jysoo Lee^(1,2) and Joel Koplik⁽²⁾

⁽¹⁾ Department of Physics, Seoul National University
Seoul 151-742, Korea

⁽²⁾ Benjamin Levich Institute and Department of Physics
City College of the City University of New York
New York, NY 10031

October 3, 2018

Abstract

We use Stokesian Dynamics simulations to study the microscopic motion of particles suspended in fluids passing through porous media. We construct model porous media with fixed spherical particles, and allow mobile ones to move through this fixed bed under the action of an ambient velocity field. We first consider the pore scale motion of individual suspended particles at pore junctions. The relative particle flux into different possible directions exiting from a single pore, for two and three dimensional model porous media is found to approximately equal the corresponding fractional channel width or area. Next we consider the waiting time distribution for particles which are delayed in a junction, due to a stagnation point caused by a flow bifurcation. The waiting times are found to be controlled by two-particle interactions, and the distributions take the same form in model porous media as in two-particle systems. A simple theoretical estimate of the waiting time is consistent with the simulations. We also find that perturbing such a slow-moving particle by another nearby one leads to rather complicated behavior. We study the stability of geometrically trapped particles. For simple model traps, we find that particles passing nearby can “relaunch” the trapped particle through its hydrodynamic interaction, although the conditions for relaunching depend sensitively on the details of the trap and its surroundings.

1 Introduction

The transport of particulate suspensions through porous media is a process with numerous industrial applications such as deep bed filtration [1, 2, 3, 4], hydrodynamic chromatography [5], migration of fines [6], ground water contamination [7], the flow of dilute stable emulsions [8], and hindered diffusion in membranes [9]. In order to understand the behavior of these systems, one often needs to know the microscopic, or “pore-scale” behavior of the suspended particles. Consider the example of deep bed filtration, where a suspension is injected into a filter made of porous material, in the hope that the suspended particles will be collected in the filter while clear(er) fluid passes through. A filtrate particle flowing through the pore space may be trapped by the geometric constraint of reaching a pore smaller than its diameter, or by other adhesive mechanisms such as electrostatic or van der Walls forces. Realistic porous media have an intricate randomly-sized and randomly-interconnected pore space with highly nontrivial flow paths. The degree to which suspended particles choose trajectories in the pore space with or without small constrictions, or tend to be attracted or repelled by the walls, or move towards or away from the other suspended particles will determine the dynamics of the filtration process. Recent experiments [10, 11] which focus on such microscopic particle behavior in filtration clearly illuminate how such pore-scale details can change the macroscopic properties of the system.

A useful way of describing the porous medium and particulate motion therein is to note that the pore space of a material like a random sphere pack involves relatively large open regions connected by relatively narrow channels: pores and throats, respectively [12]. A typical pore is connected to several others through the throats. The streamlines for fluid flow or the paths taken by suspended particles (in the absence of wall adhesion mechanisms) are then roughly unidirectional within the throats but branch at each pore, corresponding to the different connected neighboring pores which are accessible. A key issue for microscopic particulate motion is the “junction rule”: when a suspended particle reaches a pore, which of the neighboring pores does it choose to move towards next.

The necessity for such information is evident when constructing a quantitative description for the system. Consider, for example, the network model for filtration, which models a filter medium as a ball-and-stick network of nodes interconnected by channels [13, 14, 15, 16]. The trajectory of the suspended particles in the network is largely determined by the motion of the particles at the nodes, which is specified by the junction rule. Furthermore, the interaction between two nearby particles has been experimentally found to be important [10, 11]. For example, a particle which is apparently trapped at some point in the pore space may escape from the trap if another suspended particle passes nearby. This effect can significantly change the distribution of the trapped particles, and such information must be included in the model. The problem which motivates this work is that very little quantitative information on these crucial effects is available. For the junction rule, there have been studies on the related problem of red cells passing through tube hematocrits [17, 18, 19, 20, 21], where similar but different geometries were considered. In the filtration case, only rough estimates exist for both the junction probabilities and for the escape rate of trapped particles [10, 11].

In this paper, we study the microscopic motion of particles suspended in a fluid passing through a porous medium, using Stokesian Dynamics (SD) computer simulations [22]. We construct our model porous media by fixing the positions of a set of spheres, representing the grains of the porous medium, and allowing other particles, representing the filtrate, to move through this fixed bed. The original SD code, which simulated only mobile particles, was modified appropriately to handle fixed particles as well. Given that we are interested here

in relatively large non-colloidal particles, whose size is in the micron range, Brownian forces are not included in the calculations. Using this methodology, we describe the filtrate motion at junctions in two and three dimensional model porous media in terms of a quantity called the fractional particle flux (FPF). At a given pore, the FPF for any subsequent connected channel is defined as the fraction of particles choosing it out of all possible exit channels. We find that it is a good approximation to assume that the FPF of a channel is proportional to its cross-sectional area. Although this result agrees with one's simplest intuitive expectation, we are not aware of any previous quantitative verification.

A suspended particle may spend a relatively long time in a pore before proceeding to an exit channel. To quantify this effect we have also measured the “waiting” time for a particle passing through two and three dimensional model porous medium, and also for a mobile particle passing near one fixed particle. These calculations show that the waiting time is dominated by the two particle interaction – that between the mobile particle and fixed particle which divides the two exit channels. We also present an approximate analytic calculation for the waiting time, which is consistent with the numerical results. We further study the effect of another mobile particle on “hesitating” particles – those near bifurcating streamlines with large waiting times. The resulting motion of the two particles displays an unexpectedly rich range of possibilities, such as “push toward”, “push away”, “turn”, and “lead”, which we describe in more detail below.

Another important result is the condition under which geometrically trapped particles escape from the trap by the perturbation of a “bypassing” particle – another suspended particle passing nearby. We construct simple traps consisting of two and three fixed particles in two and three dimensions, respectively, and place a mobile particle in the trap. In agreement with observations, We find that a bypassing particle can “relaunch” the trapped particle based upon only hydrodynamic interactions. We determine the trajectories of the mobile particles which cause relaunching for the parameters characterizing the trap. We find that the condition for the relaunching depends not only on the geometry of the trap, but also on the surroundings. We then study the condition for the relaunching in a two dimensional model porous medium, and obtain qualitatively similar results.

2 Stokesian Dynamics

Stokesian Dynamics (SD) is a numerical method to dynamically simulate the behavior of solid particles suspended in a viscous fluid at zero Reynolds number [22], based on the resistance matrix description of particle motion in creeping flow [23]. When the Reynolds number based on the particle length scale is negligible, the generalized hydrodynamic forces \vec{F}^H exerted on the particles in a suspension are

$$\vec{F}^H = -\mu R_{FU} \cdot (\vec{U} - \vec{U}^\infty), \quad (1)$$

where the components of \vec{U} are the generalized particle velocities, \vec{U}^∞ is the ambient flow velocity evaluated at the particle centers, and we have assumed that there is no bulk shear flow. The term generalized means that both translational and rotational components are included: the velocity vector contains angular velocity components, and torques are included in the force vector, so that \vec{U} and \vec{F}^H have $6N$ components, where N is the total number of the particles. R_{FU} is the configuration dependent resistance matrix that gives the hydrodynamic forces on the particles due to their motion relative to the fluid. The inverse of the resistance matrix is the mobility matrix M_{FU} .

We briefly describe the calculation of R_{FU} in the SD method; a detailed discussion can be found in [22]. The force density on the surface of each particle is expanded in a series of multipole moments, where terms higher than quadrupole are ignored. The far field (large interparticle distance) value of the mobility matrix M_{FU} is expressed in terms of these moments. We invert M_{FU} to get the form of the resistance matrix R_{FU} relevant to the far field region. We then add near field (short interparticle distance) lubrication terms to the matrix. The resulting matrix R_{FU} is accurate both for far and near fields, but not necessarily for intermediate distance. In order to determine accurate values of R_{FU} at intermediate distance, Stokes equation is solved numerically for the system of two spheres with various separations. The numerical values of R_{FU} from the simulations are included in the present code.

Neglecting inertia, the total force on each particle is zero,

$$\vec{F}^H + \vec{F}^P = 0, \quad (2)$$

where \vec{F}^P are the non-hydrodynamic forces acting on the particles, which we specify presently. Combining Eqs. (1) and (2), one can calculate the velocities of the particles, and from the velocities, one can calculate the positions of the particles at a short time later. For this new configuration, the velocities can again be calculated, from which a new configuration can again be generated, and this process can be repeated to generate the trajectories of the particles. In this paper we wish to apply this method to the study the flow of suspensions through small subregions of rigid porous media. We construct a model porous medium by fixing the positions of certain particles to be at chosen locations, which requires some modifications of the SD method. The basic equation (1), the integration method for the (force free) moving particles, and the resistance matrix remain unchanged. However, a further requirement $\vec{U} = 0$ is required for the fixed particles, and in effect we will choose the value of an appropriate non-hydrodynamic force to impose this condition.

In the original SD formulation the velocities of the particles are determined by calculating \vec{F}^H from the force-free condition Eq. (2), and inverting Eq. (1). To fix particle's position, we apply an additional "gluing force" to balance hydrodynamic and other non-hydrodynamic forces. The problem is that the value of the gluing force is given only as a part of the solution of the problem, and we cannot simply invert Eq. (1) to obtain the velocities. We instead calculate the velocities by a recursive method. For given values of the gluing forces, one can calculate the velocities of all the particles by inverting Eq. (1). The resulting velocities are, in general, not the correct solution of the problem, that is, the velocities of the supposedly fixed particles are not equal to zero. We define Σ as the sum of the squares of the speed of the fixed particles, which is then a function of the gluing forces. The correct solution is obtained for the values of the gluing forces which makes $\Sigma = 0$, and since it is a non-negative quantity, the problem is to find the global minimum of Σ in the parameter space of the gluing forces. In other words, the problem becomes the minimization of a function, and the method of the steepest descent [24] is effective. In practice, we begin the iterative solution by using the gluing force from the previous time step, and deem that a solution is obtained when the average speed of the fixed particles is less than 10^{-5} of the ambient velocity. Fortunately, it turns out that Σ is a smooth function of the gluing forces, and does not contain other local minima, and typically 50 iterations suffice at each timestep.

To check the code, we examined a few simple two-particle configurations where an analytic solution is available. At present, only three-dimensional SD codes for monodisperse particles exist, and in the remainder of this paper, the radius of all particles is set to 1. First, we

consider head-on collisions, where we fix a particle at $(0, 0, 0)$ and place a moving particle at $(-r, 0, 0)$ in an ambient velocity field $\vec{U}^\infty = (1, 0, 0)$. (In all cases considered in this paper, no ambient angular velocity is applied, and since we are interested in the trajectories of spheres, for the most part we suppress the discussion of their individual angular velocities.) Our numerical results for the velocities are compared with those obtained analytically using the expression for the resistance matrix R_{FU} given in [25]. The two velocities agree to within 10^{-3} percent for both near and far fields. We then consider tangential motion by placing the moving particle initially at $(0, r, 0)$, without changing the other parameters. The quality of the agreement is similar to the head-on collision case. Another check is whether the solutions from the simulations exhibit required symmetries. We consider placing the moving particle initially at $(\pm x_0, y_0, 0)$, with the fixed particle and ambient flow field as above. From the obvious geometrical symmetries of this system, the x velocity, the absolute values of the y velocity and the z angular velocity should be the same, but the signs of the y velocity and the z angular velocity should be reversed for the two settings. For several combinations of x_0 and y_0 , we confirm that the solution indeed possesses the required symmetry. Lastly, we also check the dependence of the solution on the size of the computational domain. A periodic boundary condition is applied in each direction. We find that the linear size of 10,000 is enough to ensure that the effect of the boundary is negligible.

Particles in an inertialess suspension cannot overlap with or even touch each other, since the radial component of the lubrication force diverges when two particles approach. In the simulation, however, we find that the particles do overlap at times, due to the following numerical subtlety. When a moving particle approaches a fixed one, at sufficiently small interparticle distances the lubrication force indeed becomes large, and it pushes the particle away. However, since the force grows slowly, the distance at which the repulsion occurs often is very small. In our simulation, we find that this distance is typically smaller than 10^{-13} , and in principle one has to calculate the trajectory of the particles to extremely high precision. The problem is that the simulation time with this high accuracy is enormous: double precision computations are inadequate, and quadruple precision variables are needed, and furthermore the time step has to be kept very small: less than 10^{-4} . The CPU time required for even a two particle simulation at this accuracy exceeds 50 hours on a DEC AlphaStation 500/500, so such an SD simulation in a model porous medium is not feasible.

This type of simulation is not only practically impossible, but also not at all physical. The surface roughness of ordinary solid particles is typically 10^{-3} to 10^{-2} of the radius [26]. As a result the particles are not exactly spherical, and their flow behavior changes significantly when the two particle separation is at the scale of the roughness [27]. One semi-physical way to include the effects of roughness is to add an extra repulsive force at very short distances [28]. In this paper, we instead follow the simpler procedure of Phung and Brady [29], who on one hand introduced a cutoff in the resistance matrix computation, and on the other simply ignore small overlaps. When interparticle gap is smaller than the cutoff value of 10^{-5} , the value of R_{FU} at the cutoff is used. Accidental overlaps are allowed, provided the overlap distance is smaller than 10^{-3} .

3 Fractional Particle Flux

Most pores in typical porous media have more than one exit channel connected to them, and the path taken by a particle in such a pore in proceeding to the next one depends in detail on microscopic variables such as the detailed local geometry, the particle's precise location,

and the flow field (which in turn depends on the location of the other particles). It is not feasible to study more than a small subregion of a porous medium in such fine detail, and it is useful to construct a more tractable model based on a network of nodes and links. A key ingredient is such a coarse-grained description is the fraction of particles passing through a given exit path, averaged over some of the microscopic variables. We refer to this quantity as the fractional particle flux (FPF).

Although the FPF is important in understanding porous media transport in general and processes such as filtration in particular, we are not aware of any direct measurement of this quantity. Although it is possible to follow the motion of a suitably tagged suspended particle in some detail through a laboratory porous medium, one would have to map out the microscopic pore space as well, and the practical difficulties are evident. A related problem which has received some quantitative study is the flow of red cells passing through tube hematocrits. When a tube hematocrit bifurcates to two or more smaller tubes, a blood cell has to choose a tube at the junction. The fractional red cell flux is of great importance in determining red cell distribution among the microvessels, and there exist several direct and indirect measurements of it [17, 18, 19, 20, 21]. The essential problem in these two systems is the same, but their geometries are a bit different and blood cells are deformable, which may result in different qualitative behaviors of the FPF.

We construct model porous media with fixed particles in two and three dimensions. First, we consider a two dimensional medium, where particles are confined to a plane, immersed in a three dimensional fluid. Although a two dimensional medium is not realistic, it allows us to study more detailed properties (note that computation time in SD simulations increases roughly as the square of the number of particles). Fortunately, we shall see that its qualitative behavior does not differ from that of a three dimensional medium, which we discuss later. The medium consists of the 11 fixed particles shown in Fig. 1(a). The centers of all particles are in the $z = 0$ plane, and we choose the coordinates of the lower left particle to be the origin. The “lattice constant” a is the distance between neighboring particles in the same column, and it also is the distance between neighboring columns. The middle column can be shifted vertically, and we choose the y coordinate of the center particle to be $y_c + b$, where $y_c = 3a/2$. We call the system, characterized by two parameters a and b , as the “2d-11” geometry. Recall that the current code can handle only monodisperse particles whose radius is taken as 1. The ambient flow field is $(1, 0, 0)$ in all cases, unless stated otherwise. We insert a moving particle at $(-2, y_c + d, 0)$, with $-a/2 < d < a/2$, just upstream of the first column (Fig. 1(b)). After the particle reaches the node behind the first column, it will proceed to either channel A or B depending on the initial parameter d .

Assuming that the distribution of the particle along the starting line ($x = -2$) is uniform [30], we can calculate the FPF from the range of d within which the trajectory of the particle passes through channel A (or B). The FPF for a channel is often plotted against the fractional flow rate through the channel, but in the present simulation the flow rate of a channel is difficult to calculate. We use the fractional channel width (FCW) instead. We define W_i as the width of the y interval corresponding to channel i within the unit cell $[y_c - a/2, y_c + a/2]$, as shown in Fig. 1(b). The FCW of channel i is defined as W_i normalized by the lattice constant a .

We consider three values of the lattice constant, $a = 4.25, 4.5$, and 5.0 , and we also vary the fractional channel width by changing b , using five values of b for each a . For a given geometry, determined by a and b , we can measure the FPF of a channel by studying the trajectories of the particles starting from different locations characterized by d . Note that

we can determine the FPF with less effort by focusing on a neighborhood of the value of d at which the trajectory of the particle terminates at the center particle. The calculation of a typical trajectory requires about 4 CPU hours on a workstation. About 15 trajectories are needed to determine the FPF for a given geometry with fair accuracy. The FPF for the channel A are shown against its FCW in Fig. 2. In this geometry, the FPF for FCW less than $1/2$ can be determined simply by symmetry.

The most prominent feature of the figure is that all the curves lie very close to the line: $\text{FPF} = \text{FCW}$. In other words, it is a good approximation to distribute particles in proportion to the exit channel width. Small, but finite deviations from the curve are observed, especially for large FCW. Somewhat similar behavior is observed in simulations of the flow of red blood cells at a capillary bifurcation [21], but there are two noticeable differences. In the blood cell case, the FPF is larger than FCW for large FCW, in contrast to the present case. By inspecting the trajectories, it seems that the difference is caused by the difference in the local geometry around the junction. Another difference is that in the present case, the amount of the deviation increases as a increases, in contrast to the cell case. This is a bit puzzling, since we expect the FPF to follow the relative width for larger lattice constants. Further simulations indicate that the deviation shows a complicated dependence on a , before beginning to decrease for larger values, $a > 10$.

We next study a model three dimensional porous medium, consisting of 13 fixed particles, in three layers, forming a deformable hexagonal close packed (hcp) structure. There are first and third layers containing three particles each, and a second (middle) layer with seven particles, as shown in Fig. 3(a), where the layers are stacked in the x -direction normal to the plane of the figure. The y and z coordinates of the particles in the first and third layers are in register, while the middle layer can be translated in its plane to produce a family of porous structures. Specifically, the y coordinate of the center particle in the second layer lies in the dotted (center-)line of the first layer, and is shifted in the z direction by a variable amount b . When $b = 0$ the orthocenter (small circle) in the first layer coincides with the center particle in the second layer, and the particles form precisely a hexagonal close packed cell. The second parameter describing the geometry is the distance between nearest neighbor particles in the same layer, the lattice constant a . The interlayer distance is fixed at $a(2/3)^{1/2}$ in all cases studied. This system is referred to below as the “3d-13” geometry.

The ambient flow again has unit strength in the x direction normal to the layers. We insert a mobile particle in front of the gap in the first layer and, depending on its initial coordinates, it will eventually be carried around the central particle in the second layer and proceed to one of the exit channels A, B or C shown in Fig. 3(b). The initial y and z coordinates of the mobile particle lie within the “unit cell”—the largest triangle in Fig. 3(b), where the projection of the particles to the $y - z$ plane is shown. Again, the question is the fractional particle flux through each channel. Due to symmetry, the FPFs of channels A and B are identical, and all three fluxes add to unity, so it suffices to give the FPF of channel C. As in the previous simulation, calculating the FPF involves finding the ranges of initial coordinates such which the trajectory of the mobile particle passes through channel C. However, a rather larger number of trajectories for a given cell, 30, are required here, so we consider only the case $a = 10$, and the four values $b = -2, 0, 2, 4$. The calculation of one trajectory now requires about 6 CPU hours.

The measured FPF for channel C is plotted against its fractional channel area (FCA) in Fig. 4. The FCA of channel i , which is an analog of the FCW in three dimensions, is defined as the projected area of the triangle W_i , normalized by the area of the unit cell—

$\sqrt{3}a^2/2$. The FPF curve lies again very close to the FPF = FCA line, and the number of particles passing through a channel is to a very good approximation proportional to its channel area. Small deviations from the FPF = FCA line can be seen, similar to those in the 2d-11 geometry.

From these simulations of motion in two and three dimensional porous media, we find that the fractional particle flux for a channel is, to a good approximation, proportional to its channel width (in 2d) or area (in 3d). Since a particle at a given initial location always passes through the same channel, we expect the “mixing” at the node is not significant, which is consistent with observations in the flow of red blood cells [21]. A contrasting assumption is commonly made for the motion of passive tracers in porous media flow. The alternative “complete mixing” rule assumes that a tracer particle (effectively, a particle small enough not to disturb the flow field) in a pore chooses an exit pore based only on the relative flux there, independent of its position of entry into the pore. Evidently, this assumption is reasonable only if the local Péclet number is small enough for the particle to diffuse substantially within the pore and lose memory of its initial streamline.

4 Waiting Time near a Junction

Consider a particle in a pore with, for example, two possible exit paths, In the absence of suspended particles, the flow field will have a dividing streamline terminating on the fixed particle, and a passive fluid particle on this streamline would reach the fixed particle only after infinite time. Suspended particles will alter this picture somewhat, but there will be a single mathematical trajectory which reaches the fixed particle after infinite time, and when a particle lies close to the line its velocity will be small, and it will “wait” in this pore before proceeding to the next. Such behavior was observed in the simulations of a particle passing through a bifurcating tube [21]. Here, we study in detail the parameter dependence of the waiting time for model porous media.

We first study the waiting time numerically for the 2d-11 geometry. A mobile particle is inserted at $(-2, y_c + d)$, just upstream of the first layer (see Fig. 1(b)). This particle may dally in front of the center particle which divides channels A and B, and to quantify this effect we define the waiting time T_w as the time the mobile particle is in the interval $(x_c - 2) - 0.1 < x < (x_c - 2) + 0.1$, where x (x_c) is the x coordinate of the mobile (center) particle. In Fig. 5(a), we plot T_w against d for $a = 4.5$ and five values of b . (For other values of a , 4.25 and 5.0, the qualitative features of the results are unchanged.) As seen in the figure, T_w is sharply peaked around a b -dependent value d_{peak} , where waiting times as much as 100 times larger than the large- d values are seen. Furthermore, the peaks are essentially all the same, as seen if we superpose the individual peaks by plotting T_w against $d - d_{\text{peak}}$ in Fig. 5(b), and noting that they roughly collapse to a single curve. Since the individual peaks intuitively correspond to the moving particle stagnating near the dividing fixed particle in the second layer, and do not seem to depend on exactly where the latter is located, one suspects that the waiting time is only sensitive to the two particle interaction between the mobile and the center particles.

Similar behavior is found in three dimensions. In the 3d-13 geometry, we place a mobile particle in front of the first layer, along the vertical line passing through the center particle of the second layer in Fig. 3(b). Here, we define d as the difference in z coordinate between the mobile particle and the center particle of the second layer, and the waiting time T_w as the amount of time the mobile particle spends in $x_c - 2 - 0.1 < x < x_c - 2 + 0.1$, where x

(x_c) is the coordinate of the mobile (center) particle. In Fig. 6(a), we show T_w for $a = 10$, and four values of b . These curves are similar to those for the 2d-11 geometry and, when shifted by their peak positions d_{peak} , collapse again to the single curve in Fig. 6(b). The collapsed curve is very similar to that of the 2d-11 geometry, further supporting the idea that the effect of the particles surrounding the mobile and center particles is not significant.

To pursue this simplifying idea, we consider the interaction of a mobile particle with only a single fixed particle. We fix the latter at the origin, and place a mobile particle initially at $(-5, d, 0)$. We again define the waiting time T_w as the time the mobile particle spends in $-2.1 < x < -1.9$. In Fig. 7, we plot the waiting time for the two particle system in a log-log plot, along with those of the 2d-11 ($a = 4.5, b = 0$ and $b = 0.45$) and the 3d-13 geometries ($a = 10, b = 0$). Aside from a difference in overall scale, the waiting time variation for the different cases is identical, verifying that the two-particle interaction is the dominant factor. (The origin of the difference in time scale is simply a matter of a different superficial velocity: the asymptotic velocity far from the packing is the same in all cases, so the scale of the velocity near the two particle subsystem will depend on the superficial velocity within the packing. The 2d-11 geometry is most closely packed, has the lowest permeability and lowest velocities, and the longest times. The two particle system is the most open and has the highest velocities and shortest times.)

The two particle system can be treated analytically. We fix a particle at the origin and insert a mobile particle at $(-2 - d, 0, 0)$, where $0 < d \ll 1$ for the long waiting time limit. The ambient velocity field is $U^\infty = (\cos \theta, \sin \theta, 0)$, and the mobile particle moves in the $z = 0$ plane (Fig. 8). From Eq. (1), the forces on the particles are

$$\begin{pmatrix} \vec{F}^1 \\ \vec{F}^2 \end{pmatrix} = -\mu \begin{pmatrix} A_{11} & A_{12} \\ A_{21} & A_{22} \end{pmatrix} \begin{pmatrix} \vec{U}^\infty - \vec{U}^1 \\ \vec{U}^\infty - \vec{U}^2 \end{pmatrix}, \quad (3)$$

where \vec{F}^i and \vec{U}^i are the hydrodynamic force and velocity acting on particle i , and we ignore the z components of these vectors. At these near-touching distance, the contribution from the linear motion of the particle is much larger ($1/\xi$, where ξ is the gap width) than that from the rotation ($\ln \xi$), so we ignore the contribution of rotation of the particle to the forces. Imposing the force free condition $\vec{F}^1 = 0$ and the fixing condition $\vec{U}^2 = 0$,

$$\begin{aligned} (X_{11}^A + X_{12}^A) U_x^\infty &= X_{11}^A U_x^1 \\ (Y_{11}^A + Y_{12}^A) U_y^\infty &= Y_{11}^A U_y^1, \end{aligned} \quad (4)$$

where X_{ij}^A and Y_{ij}^A are two particle resistance functions [25]. When the particles nearly touch,

$$U_y^1 = \left(1 + \frac{Y_{12}}{Y_{11}}\right) U_y^\infty \simeq \left(1 + \frac{Y_{12}}{Y_{11}}\right) b, \quad (5)$$

where b is the impact parameter as shown in Fig. 8. Substituting the near-field form of the resistance matrices [25] we have

$$U_1^y \simeq -\frac{3(A_{11}^Y(1) + A_{12}^Y(1))}{\ln \xi} b. \quad (6)$$

Here, $A_{ij}^Y(1)$ are known constants satisfying $A_{11}^Y(1) + A_{12}^Y(1) > 0$, and ξ is the gap distance between the two particles. Since $\ln \xi$ is a slowly varying function, we can ignore its variation. The above equation becomes,

$$U_1^y \simeq -\alpha b, \quad (7)$$

where α is a new constant. Note that the approximations made are valid at near-touching distance, and within a certain range of ξ . We can estimate the waiting time as that required for particle to proceed from $y = y$ to $y = y + \delta y$. Then,

$$T_w \sim \int_y^{y+\delta y} \frac{1}{U_1^y} dy \sim \frac{1}{\alpha} \ln\left(1 + \frac{\delta y}{y}\right), \quad (8)$$

where we use that $b \simeq y$ near touching distance.

We determine α and δy from the least square fit of the Eq. (8) to the measured time for the two particle simulation. The waiting time from Eq. (8) with these parameters ($\alpha = 0.166$ and $\delta y = 0.329$) is shown along with measured waiting times in Fig. 7. The overall shape of the analytic curve agrees very well with the numerical computations for small values of the impact parameter, while the deviation at large d is expected, since Eq. (8) holds only at if the particles nearly touch.

Given the agreement between the behavior of the waiting times in various systems, it is reasonable to conclude that two-body interactions control the tail of T_w . Two qualifications are in order, however. The porous systems we have considered are relatively “open”, and it is evident which fixed particle the mobile one interacts with. In a densely packed porous medium, particularly one involving heterogeneous shapes and sizes, some ambiguity may be present. Secondly, one may ask about the effects of the other mobile particles. When the suspension is dilute, one may distinguish between the case of a mobile particle approaching another that is waiting in a pore, the subject of the next section in fact, and the effects of perturbations in the velocity field induced by more distant suspended particles. An accurate treatment of the latter question requires a much more extensive set of additional simulations than we are able to provide at this time, but an approximate treatment may be given by considering the effect of *noise* on the waiting time. We used the 2d-11 geometry, with $a = 4.5$ and $b = 0.9$, and oscillated the particle at the lower left to provide a perturbation on the trajectory of the mobile particle. The amplitude of the oscillation was 1 and its frequency is 0.1, comparable to the time scale of the particle motion. The measured waiting time with noise is not substantially different than without, except that the peak is somewhat rounded, and we conclude that perturbations of this form do not seem to alter the waiting time significantly.

5 Perturbation of a Waiting Particle

As discussed in the previous section. a particle may spend significant amount of time around a junction, and we now consider the perturbations induced by other mobile particles in the vicinity, *i.e.*, the effect of a “bypassing” particle on a “waiting” particle. This represents one special case of the hydrodynamic interaction between two mobile particles in a porous medium, but a particularly important one in applications such as deep bed filtration where slow particles are likely to adhere or be left behind in the filter.

In the previous section, it was shown that the dynamics of particles moving slowly through pores is controlled by two particle interactions, so we first consider the effect of a third mobile particle on a simple two-particle system. We fix a particle at the origin, and insert mobile particles at $(-2.2, d_w, 0)$ and $(-5, d_p, 0)$. The first mobile particle would wait near the fixed one if alone, and the second mobile particle perturbs it. We measure the waiting time T_w , again defined as the amount of time the waiter spends in $-2.1 < x < -1.9$.

In Fig. 9(a), we show the waiting time for $d_w = 0.1$, plotted against d_p . For large and small values of d_p , the waiting time approaches that of the unperturbed particle ($T_w \sim 10$), but the notable features in the figure are a minimum at $d_p = -0.5$ and a maximum at $d_p = 0.6$. The origin of these extrema can be understood by inspecting the trajectories of the particles. Around the value of d_p at which the minimum of T_w occurs, the perturbing particle passes below the fixed particle and it pushes the waiting particle *away* from the fixed particle. The waiting particle then easily escapes from the junction. Around the local maximum, the perturbing particle passes above the fixed particle and pushes the waiting particle *towards* it, making it harder for the waiting particle to escape from the junction.

For smaller values of d_w , the behavior becomes more complicated. We show the waiting time for $d_w = 0.01$ against d_p in Fig. 9(b). Here again, for small and large values of d_p , the waiting time approaches that of the unperturbed particle. However, there are now *three* maxima and *three* minima in the waiting time, compared to one each in the previous case. We label the minima as A ($d_p = -2.0$), B ($d_p = -0.5$), and C ($d_p = 0.6$), and the maxima as D ($d_p = -0.9$), E ($d_p = -0.1$), and F ($d_p = 2.5$). The minimum A is the “push away” case of $d = 0.1$. Around minima B and C, the waiting particle, by following the perturbing particle, escapes from the junction. The perturbing particle, which seems to form a temporary bound state with the waiting particle [31], makes it easier for it to escape. In other words, it “leads” the waiting particle from the junction. The minimum B (C) occurs when the perturbing particle leads below (above) the fixed particle. We next consider the maxima; at D, the perturbing particle initially leads the waiting particle. However, the bond between the two breaks, when the waiting particle cannot catch up to the leading particle. The waiting particle then changes its direction (“turns”), and proceeds to the opposite channel. This series of events increases the waiting time. The maximum E is due to a “head on” collision. When all three particles lie close to a straight line, we expect a large waiting time since any motion orthogonal to the line, which is essential for escape, will take time. The last maximum (F) is due to the “push toward” case of $d_w = 0.1$. As d_w is further decreased, we observe the same mechanisms in the qualitative behavior of the waiting time. We have gone as low as $d_w = 0.0001$, with no new phenomena appearing.

Next we ask whether the above “moves” are also observed in more realistic geometries, by studying the waiting time in the 2d-11 geometry (with $a = 5$ and $b = 0$). We insert one mobile particle at $(x_c - 2.2, y_c + d_w, 0)$, where (x_c, y_c) are the coordinates of the center particle. A mobile perturbing particle is placed at $(x_c - 7, y_c + d_p, 0)$, and we measure the waiting time of the first mobile particle for a few combinations of d_w and d_p . In Fig. 9(c), we plot the waiting time against d_p for $d_w = 0.0001$. The curve is not very different than the previous case of $d_w = 0.01$. There are three maxima at $d_p = -1.4, 0.4$ and 1.6 , and two minima at $d_p = -0.1$ and $d_p = 0.9$, but the waiting time does not yet approach to its unperturbed value in the current range of d_p . The origin of the extrema can also be connected to particular moves of the two particles. The three maxima are due to the “turn” of the waiting particle. The motion near the minimum at -0.1 is dominated by the “push away” move, and at the other minimum by the “lead” move. Note that in this geometry with many fixed particles, a single trajectory can contain multiple moves. For example, both the maximum at 0.4 and the minimum at 0.9 involve both the lead and turn moves. Near the maximum, the turn move gives dominant contribution to the waiting time, while the lead move dominates near the minimum.

The waiting times for the 2d-11 configuration are not exactly the same as that for the three particle configuration, not entirely surprisingly. Not only is the sequence of moves

different, but new ones are present, and it would be difficult to infer the waiting time for a realistic porous medium from these simple studies alone. It is clear that such three or multi-body interactions have a significant quantitative effect on transit times for particles through a porous medium, and this effect could at best be captured in an average way in simplified models, such as those based on network representations of porous media.

6 Relaunching of Trapped Particles

One of the important mechanisms for the capture of particles suspended in a fluid flowing through a porous medium (see, e.g., [2, 4]), is geometrical trapping (or straining), where particles are caught in constrictions smaller than their diameter. It has been observed experimentally that such particles can escape (or be “relaunched”) from the trap, due to another particle passing near the trapped one [10, 11]. These authors argue, albeit without direct evidence, that the relaunching is caused by hydrodynamic interactions between the two particles. These experiments also indicate that relaunching qualitatively changes the distribution of the trapped particles, and in particular the efficiency of a filter. Thus understanding of the relaunching mechanism and its quantitative measurement are important in understanding the long time behavior of particulate systems such as deep bed filters. We now consider this question within our model porous media, and show that relaunching does occur with hydrodynamic interaction only, and then estimate the relaunching rate.

We first study a two dimensional system, where all particles are confined to the $z = 0$ plane. We form a trap using two fixed particles, whose geometry is determined by the distance r between the two particle centers and θ , the angle between the line joining the two particle centers and y -axis (Fig. 10). The coordinates of two particles are $(\pm(r/2) \sin \theta, \pm(r/2) \cos \theta, 0)$, and the ambient flow is $(1, 0, 0)$. We insert a mobile particle in the trap, barely touching the two fixed particles as shown in Fig. 10. In the absence of additional particle, the particle remains in the trap, and its exact coordinate is determined within the SD simulation. We then insert another mobile particle at $(-5, d)$, which is carried near the trap, and ask under what conditions the trapped particle is dislodged. Typically, for given values of r and θ , there is a finite range of d where relaunching is observed: the $r = 2$ results, for example, are plotted in Fig. 11. This behavior is qualitatively reasonable, since as θ increases, the “barrier” becomes more aligned with the ambient flow. (For $r = 2$, if θ is much larger than 30° , we expect the mobile particle does not touch the lower fixed particle, and moves away from the trap even in the absence of any disturbance.) We next fix θ at 10 degrees, and study the dependence of the relaunching condition on r . We find that relaunching becomes less frequent as r increases, and none at all is observed for $r = 3$, which again can be understood in terms of the stability of the trapped particle. In order to calculate the average relaunching probability, one has to average over all possible trap configurations (over r and θ), and the trajectory of the perturbing particle (over d). A very rough estimate of the probability, based on the data similar to that above, is on the order of a few percent.

An amusing aspect of relaunching is that in the trajectories taken by the particles it is not the case, as one might expect, that the perturbing particle “pushes” the trapped one away from the trap. Rather, we find that the perturbing particle always “leads” the trapped particle from the trap (see the previous section for the precise definition of push and lead).

Next, we consider how relaunching is affected by a porous medium – the other fixed particles surrounding the trap. To this end, we replace the center particle in the 2d-11 geometry

by the two-particle trap just discussed, giving a 12-particle porous medium characterized by the lattice constant a , the vertical shift of the second layer b , the distance between two trap particles r , and the tilt angle θ . We insert one mobile particle in the trap, and a second mobile particle at $(-2, d, 0)$ just in front of the first layer. In general we find that while relaunching still occurs, the effect is noticeably suppressed by the surrounding particles. For example, if we fix $a = 8$, $b = 0$ and $r = 2$ while varying θ and d , again no relaunching is observed for $\theta = 0$, for $\theta = 10^\circ$ the d -interval for relaunching is too narrow to be worth determining and for $\theta = 20$ relaunching is observed for the interval $0.5 \leq d \leq 0.9$, narrower than in the open geometry. Again the mechanism at the individual trajectory level is that the perturbing particle leads the trapped particle away from the trap. Thus, while relaunching observed in a model porous medium as well as an open system, its likelihood is considerably reduced, by a factor of $5 \sim 10$ for these parameters. In other cases, for example significantly smaller values of a , relaunching is again suppressed if not eliminated. In qualitative terms, one might say that the surrounding fixed particles have the effects of suppressing the velocity perturbations due to the mobile particle (via porous medium hydrodynamic screening) as well as constraining the phase space available for the trapped one.

In order to check whether the dimensionality is relevant to relaunching, we considered a three dimensional triangular trap, consisting of three particles, with a mobile particle trapped in the middle, and the ambient flow field orthogonal to the triangular plane. We find relaunching occurs in a similar manner, where the trapped particle follows the “leading” particle. The relaunching rate differs from the two dimensional cases, however, and given the large parameter space involved, it is not feasible to provide a quantitative estimate of the rate for any given porous medium.

7 Summary

We have studied the microscopic behavior of particles suspended in fluid passing through a porous medium using Stokesian Dynamics numerical calculations. The porous medium was constructed by fixing the positions of certain particles in a fluid, with the appropriate modifications in the code, and the remainder were allowed to move under the action of an ambient flow and the hydrodynamic interactions due to all fixed and moving particles. We measured the fractional particle flux for two and three dimensional model porous media. We find that the FPF for a channel is, to an excellent approximation, proportional to its fractional channel width (in two dimensions) or area (in three). The details of the distribution seem to be highly dependent on the local geometry, in particular the distribution of particles at the channel entrances, so it is difficult to draw general conclusions about its form.

We examined the waiting time distribution for particles moving slowly in pore junctions, typically caused by a bifurcating flow path due to a particular fixed particle at the pore boundary. We compared the behavior of appropriate particle trajectories in two and three dimensional model porous media to motion under two-body interactions alone, treated either numerically or analytically. The results are essentially the same in all cases and indicate that the waiting time is dominated by the interaction between the mobile particle and the fixed particle which divides the possible flow paths.

We then considered the perturbations to a “waiting” particle near a junction due to a second mobile “bypassing” particle. We find that the interaction between the two particles leads to an unexpected and rich behavior, displaying several types of motions as the two mobile particles interact with each other. An important related quantity is the relaunching

rate of geometrically trapped particles, representing the likelihood that a particle caught in a geometrical trap is released by the effects of a second particle nearby. We constructed simple traps in two and three dimensions, in which particles are trapped in a constriction. We find that the trapped particles can indeed be relaunched from the trap by this mechanism, and that the relaunching rate depends sensitively on the surrounding geometry of the trap.

A principal motivation for this work is to develop computational approaches to the dynamics of processes such as deep bed filtration, where there are innumerable microscopic details, by replacing them by a coarser-grained but tractable network description. Network modeling of fluid or passive tracer flow in porous media seems to capture many of the relevant aspects [32, 33] and we have been guided by the detailed experimental observations cited above in identifying pore scale mechanisms to understand. The results in this paper have succeeded in part, in that we have shown that effects such as hydrodynamic relaunching have a firm basis, and explored many of the microscopic interactions controlling filtration dynamics. We are limited principally by the range of geometries we can construct, in particular the restriction to monodisperse particles, and by the relative slowness of SD computations in general. Future work will, we trust, alleviate these restrictions.

Acknowledgment

We thank J. Brady and T. Phung for providing the Stokesian Dynamics code, and for helping us with its use, and E. Guazzelli for extensive discussions of the filtration experiments which motivated this study. This work was supported by the Department of Energy under Grant No. DE-FG02-93-ER14327. One of us (J.L.) is supported in part by SNU-CTP and Korea Science and Engineering Foundation through the Brain-Pool program. The simulations were performed at the Systems Engineering Research Institute in Korea.

References

- [1] J. Herzig, D. Leclerc, and P. LeGoff, "Flow of Suspensions through Porous Media: Application to Deep Bed Filtration," *Ind. Eng. Chem.* **62**, 8-35 (1970).
- [2] S. Goren, "Matrix Filtration, a Tutorial," in *Physical Separations*, edited by M. Freeman and J. FitzPatrick, 535-548 (Engineering Foundation, New York, 1977).
- [3] J. Dodds, G. Baluais, and D. Leclerc, "Filtration Process," in *Disorder and Mixing*, edited by E. Guyon, J. Nadal, and Y. Pomeau, 163-183 (Klewer, Dordrecht, 1988).
- [4] C. Tien, *Granular Filtration of Aerosols and Hydrosols* (Butterworths, Boston, 1989).
- [5] E. Heftmann, ed. *Chromatography*, 5th ed. (Elsevier, Amsterdam, 1992).
- [6] K. Khilar, H. Fogler, and J. Ahlawalia, "Sandstone Water Sensitivity: Existence of a Critical Rate of Salinity Decrease for Particle Capture," *Chem. Eng. Sci.* **38**, 789-800 (1983).
- [7] C. H. Ward, W. Giger, and P. L. McCarty, eds. *Ground Water Quality* (Wiley, New York, 1985).
- [8] D. Schmidt, H. Soo, and C. Radke, "Linear Oil Displacement by the Emulsion Entrapment Process," *Soc. Pet. Eng. J.* **24**, 351-360 (1984).
- [9] M. Sahimi and V. Jue, "Diffusion of Large Molecules in Porous Media," *Phys. Rev. Lett.* **62**, 629-632 (1989).
- [10] C. Ghidaglia, L. de Arcangelis, J. Hinch, and E. Guazzelli, "Hydrodynamic Interactions in Deep Bed Filtration," *Phys. Fluid A* **8**, 6-14 (1996).
- [11] C. Ghidaglia, L. de Arcangelis, J. Hinch, and E. Guazzelli, "Transition in Particle Capture in Deep Bed Filtration", *Phys. Rev. E* **53**, R3028-R3031 (1996).
- [12] F. A. L. Dullien, *Porous Media: Fluid Transport and Pore Structure*, 2nd ed. (Academic, New York, 1992).
- [13] M. Leitzelement, P. Maj, J. Dodds, and J. Greffe, "Deep Bed Filtration in a Network of Random Tubes," in *Solid Liquid Separation*, edited by J. Gregory, 273-296 (Ellis, Harwood, 1984).
- [14] S. Rege and H. Fogler, "A Network Model for Deep Bed Filtration of Solid Particles and Emulsion Drops," *AIChE. J.* **34**, 1761-1772 (1988).
- [15] M. Sahimi and A. Imdakm, "Hydrodynamics of Particulate Motion in Porous Media," *Phys. Rev. Lett.* **66**, 1169-1172 (1991).
- [16] J. Hampton, S. Savage, and R. Drew, "Computer Modelling of Filter Pressing and Clogging in a Random Tube Network," *Chem. Eng. Sci.* **48**, 1601-1611 (1993).
- [17] P. Johnson, "Red Cell Separation in the Mesenteric Capillary Network," *Amer. J. Physiol.* **221**, 99-104 (1971).

- [18] P. Gaehtgens, A. Pries, K. Albrecht, "Model Experiments on the Effect of Bifurcations on Capillary Blood Flow and Oxygen Transport," *Pfuegers Arch.* **380**, 115-120 (1979).
- [19] J. Dellimore, M. Dunlop, P. Canham, "Ratio of Cells and Plasma in Blood Flowing Past Branches in Small Plastic Channels," *Amer. J. Physiol.* **244**, H635-H643 (1983).
- [20] G. Bugliarello, and G. Hsiao, "Phase Separation in Suspensions Flowing through Bifurcations: A Simplified Hemodynamic Model," *Science* **143**, 469-471 (1964).
- [21] D. Audet and W. Olbricht, "The Motion of Model Cells at Capillary Bifurcations," *Microvasc. Res.* **33**, 377-396 (1987), and references therein.
- [22] J. Brady and G. Bossis, "Stokesian Dynamics," *Annu. Rev. Fluid Mech.* **20**, 111-157 (1988).
- [23] H. Brenner and M. E. O'Neill, "On the Stokes Resistance of Multiparticle Systems in a Linear Shear Field," *Chem. Eng. Sci.* **27**, 1421-1439 (1972).
- [24] W. Press, S. Teukolsky, W. Vetterling, B. Flannery, *Numerical Recipes* (Cambridge University Press, Cambridge, 1992).
- [25] S. Kim and S. Karrila, *Microhydrodynamics: Principles and Selected Applications* (Butterworth-Heinemann, Boston, 1991).
- [26] J. Smart and D. Leighton, "Measurement of the Hydrodynamic Surface Roughness of Noncolloidal Spheres," *Phys. Fluids A* **1**, 52-60 (1989).
- [27] R. Davis, "Effects of Surface Roughness on a Sphere Sedimenting through a Dilute Suspension of Neutrally Buoyant Spheres," *Phys. Fluids A* **4**, 2607-2619 (1992), and references therein.
- [28] D. Dratler and W. Schowalter, "Dynamic Simulation of Suspensions of non-Brownian Hard Spheres," *J. Fluid Mech.* **325**, 53-77 (1996).
- [29] T. Phung, "Behavior of Concentrated Colloidal Suspensions by Stokesian Dynamics Simulation," Ph. D. thesis, California Institute of Technology (1993).
- [30] The assumption of the uniform distribution is, in general, not correct. We expect that, for a given geometry, the distribution can be measured by following many trajectories for large period of time. However, the distribution we measure by the method is too sensitive to small changes in the geometry, and it is not clear that such distribution can serve as a better approximation.
- [31] Bound states of two particles in a suspension with only hydrodynamic interactions were first studied by G. K. Batchelor and J. Green, "The Hydrodynamic Interaction of Two Small Freely-Moving Spheres in a Linear Flow Field" *J. Fluid. Mech.* **56**, 375-400 (1972).
- [32] H. Brenner and P. L. Adler, "Multiphase Flow in Porous Media," *Annu. Rev. Fluid Mech.* **20**, 35-59 (1988)
- [33] M. Sahimi, "Flow Phenomena in Rocks: From Continuum Models to Fractals, Percolation, Cellular Automata, and Simulated Annealing," *Rev. Mod. Phys.* **65**, 1393-1534 (1993).

Figure Captions

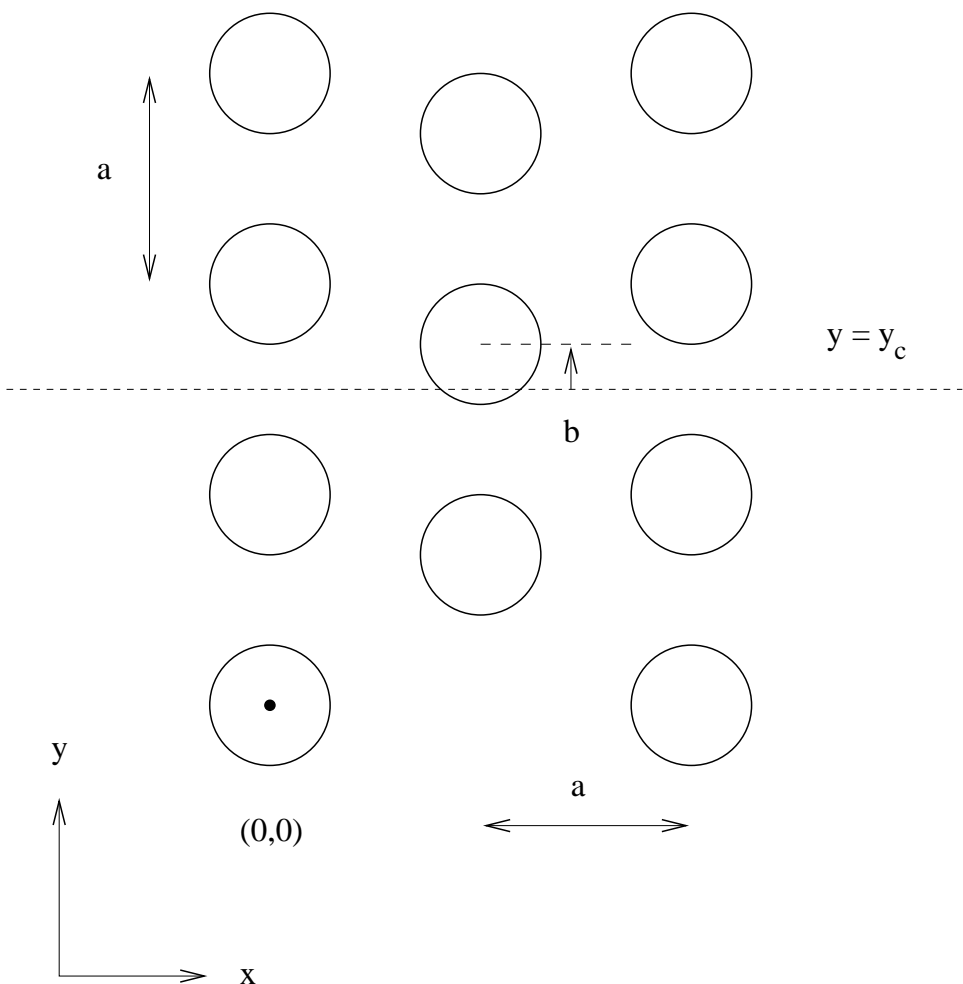


Fig. 1(a)

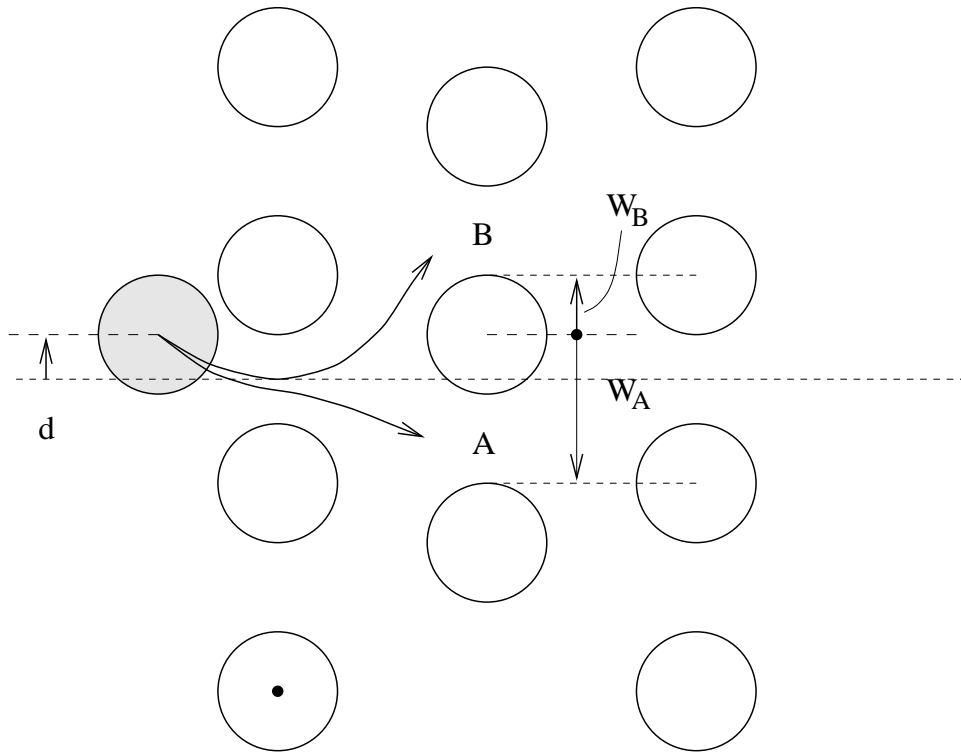


Fig. 1(b)

Fig. 1: (a) A two dimensional model porous medium consisting of 11 spheres in a plane, characterized by the “lattice constant” a and the vertical displacement b . (b) Possible trajectories A and B of a moving particle (shaded), initially at $(-2, y_c + d, 0)$, in the ambient velocity field $(1, 0, 0)$.

Fig. 2

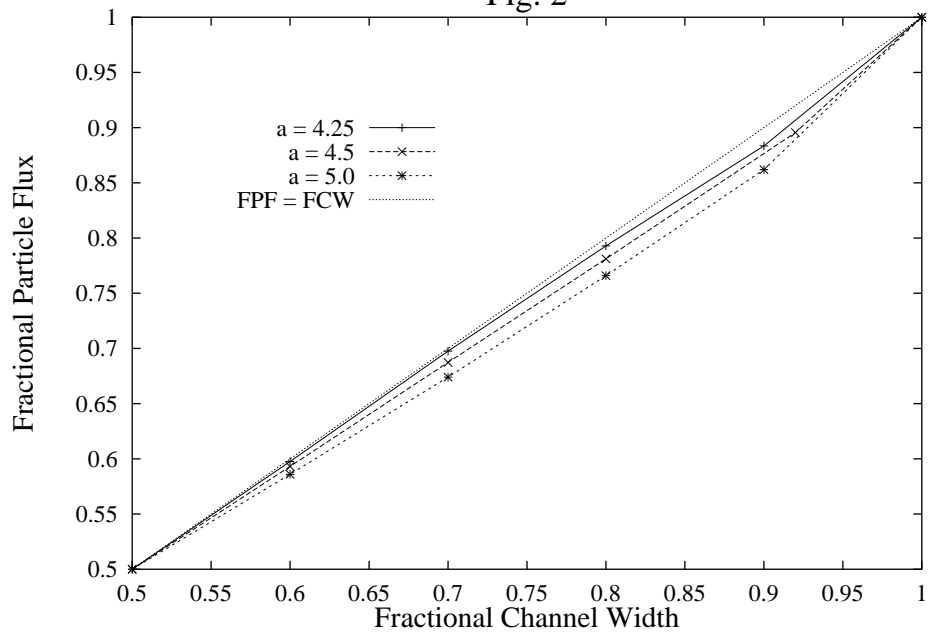


Fig. 2: The fractional particle flux (FPF) for channel A plotted against its fractional channel width (FCW) for the $2d - 11$ geometry, for $a = 4.25, 4.5$ and 5.0 . The dotted line represents $\text{FPF} = \text{FCW}$.

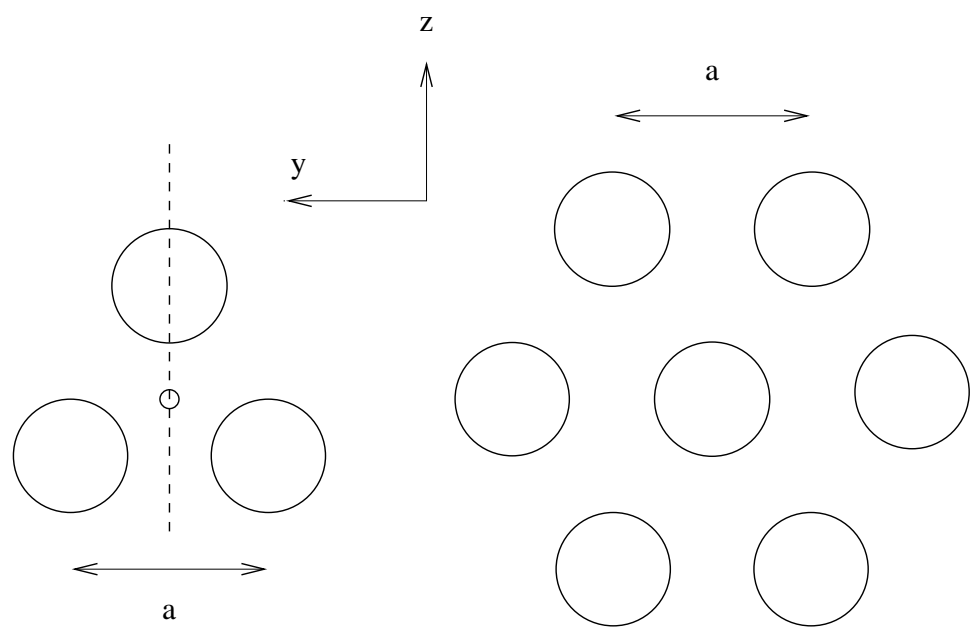


Fig. 3(a)

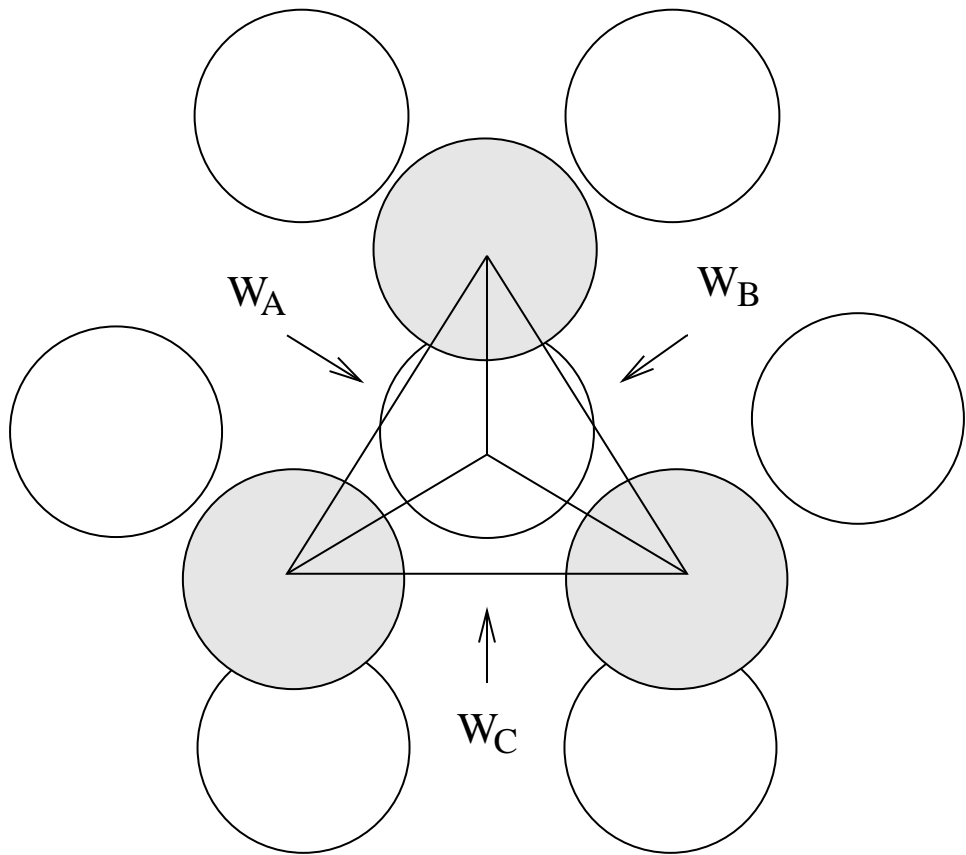


Fig. 3(b)

Fig. 3: (a) The first and second layers, respectively, of a three dimensional porous medium. The third layer is identical to the first, and they are spaced in the (out-of-plane) x direction by $a\sqrt{2/3}$, where the (in-plane) lattice constant is a . (b) A mobile particle is initially placed within the triangular “unit cell” at a small value of x , and then passes through one of the three channels (A, B or C). The figure here shows the projection onto the $y - z$ plane.

Fig. 4

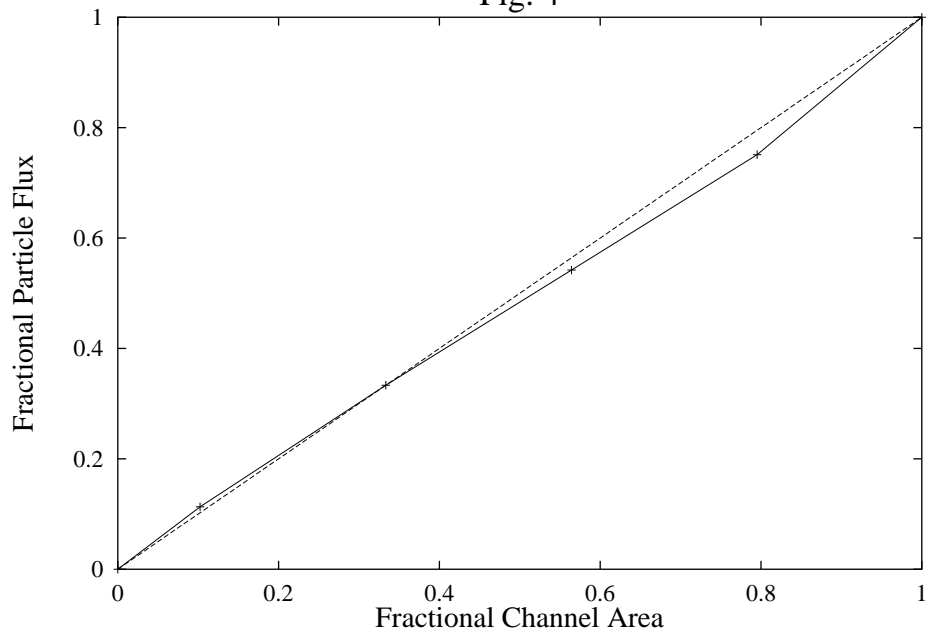


Fig. 4: Fractional particle flux (FPF) passing through channel C against its fractional channel area (FCA) for the $3d - 11$ geometry with $a = 10$. The dotted line represents $\text{FPF} = \text{FCA}$.

Fig. 5(a)

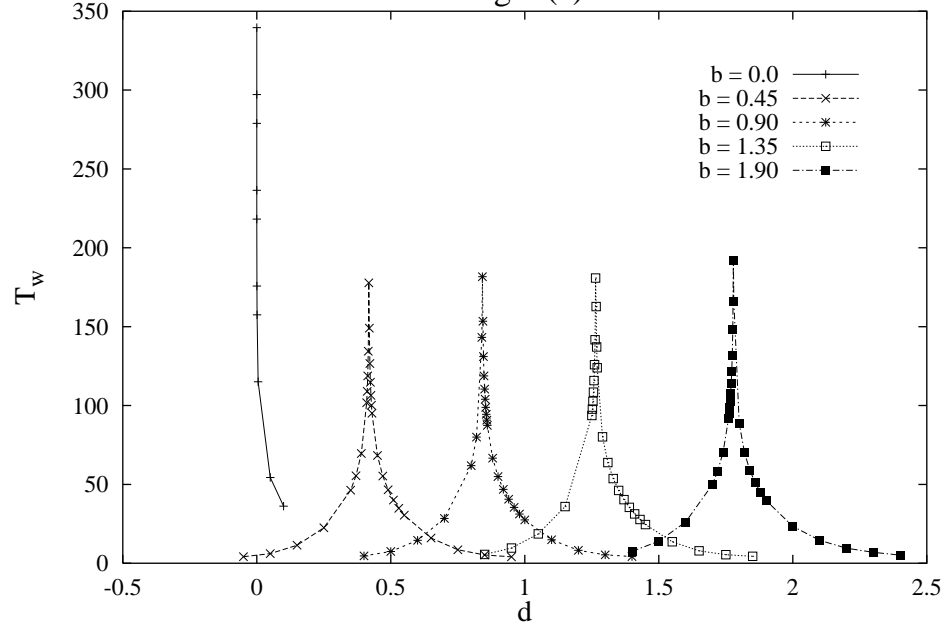


Fig. 5(b)

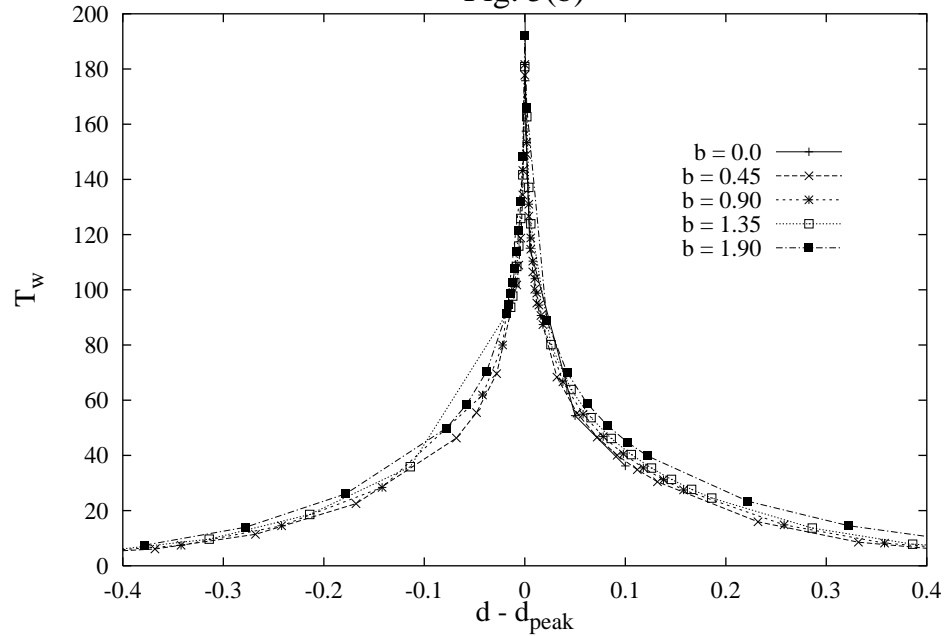


Fig. 5: (a) Waiting time T_w for the 2d-11 geometry with $a = 4.5$ and several values of b .
 (b) The curves in (a) are shifted by d_{peak} , whereupon they approximately collapse into a single master curve.

Fig. 6(a)

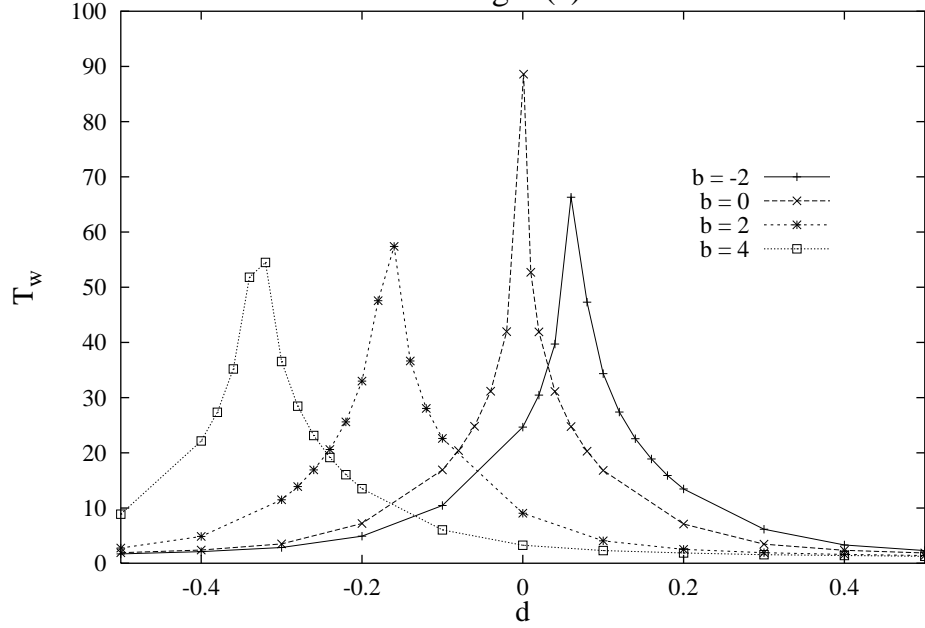


Fig. 6(b)

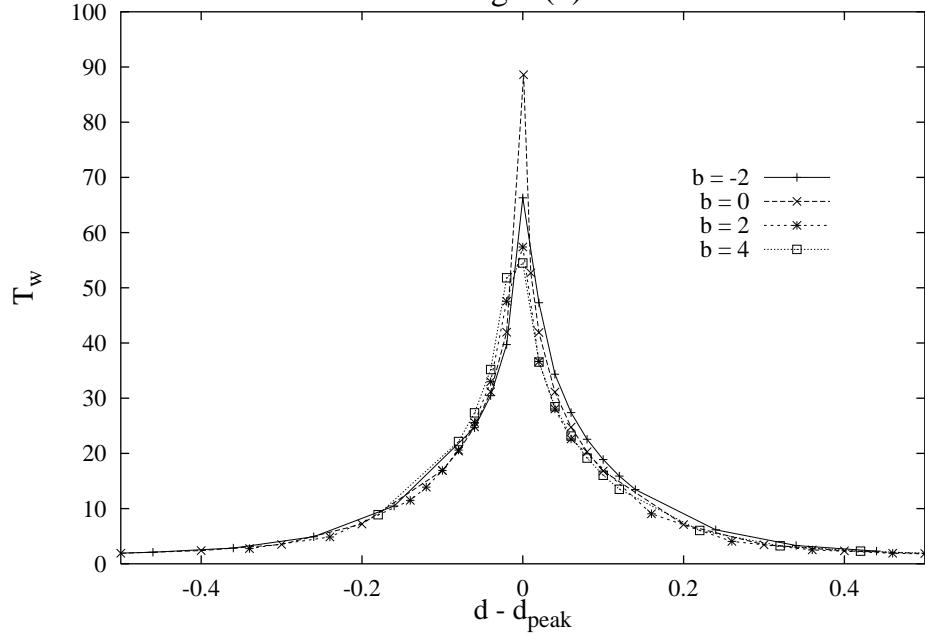


Fig. 6: (a) Waiting time T_w for the 3d-13 geometry plotted against d , with $a = 10$ and four values of b . (b) The curves in (a) are shifted by d_{peak} , and again seem to collapse to a single master curve.

Fig. 7

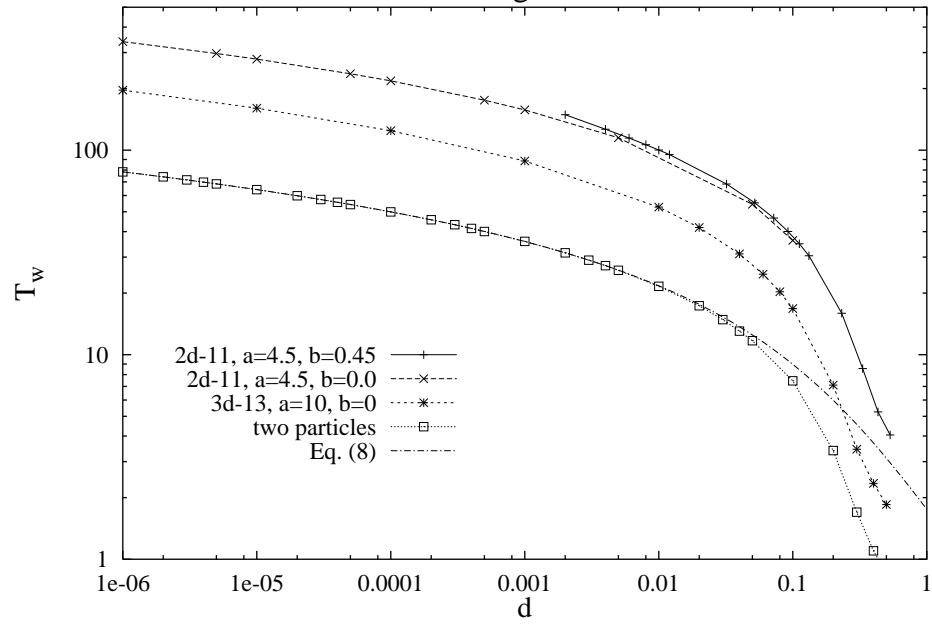


Fig. 7: Waiting time for a two particle system is shown together with those for the 2d-11 ($a = 4.5, b = 0$ and $b = 0.45$) and the 3d-13 ($a = 10, b = 0$) geometries, along with the analytic estimate Eq. (8) with $\alpha = 0.166$ and $\delta y = 0.329$.

Fig. 8(a)

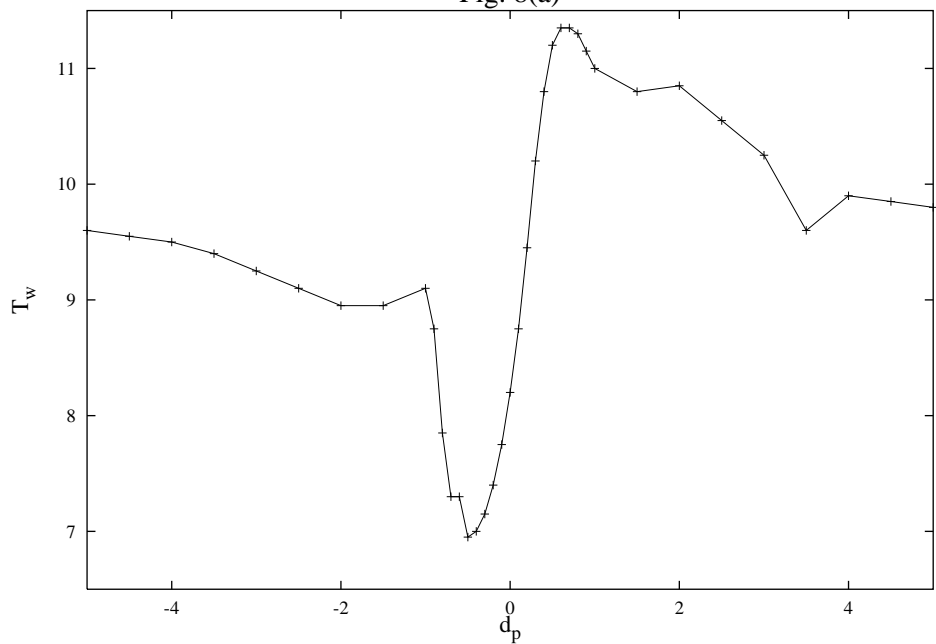


Fig. 8(b)

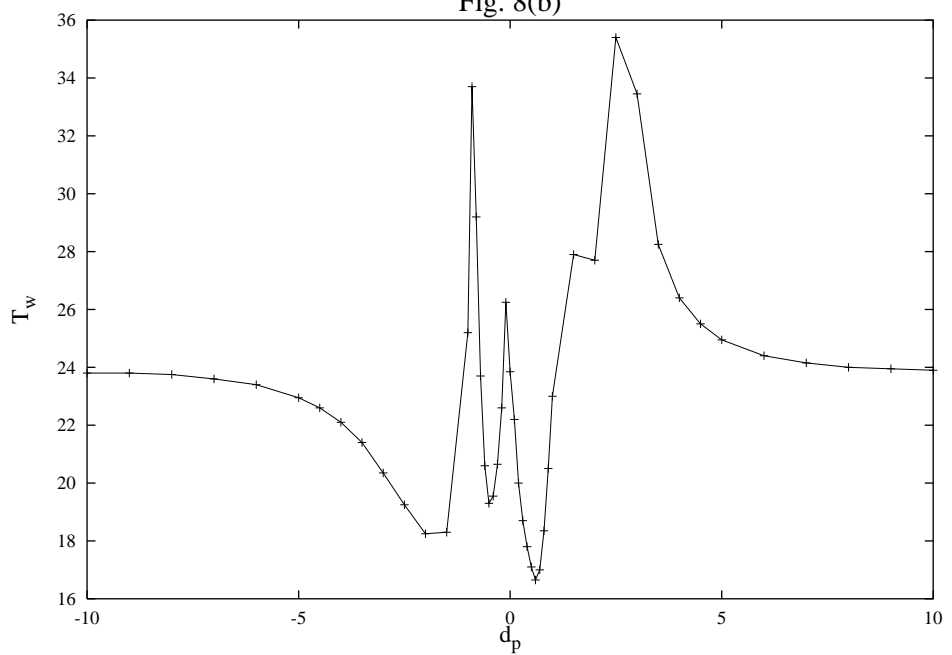


Fig. 8(c)

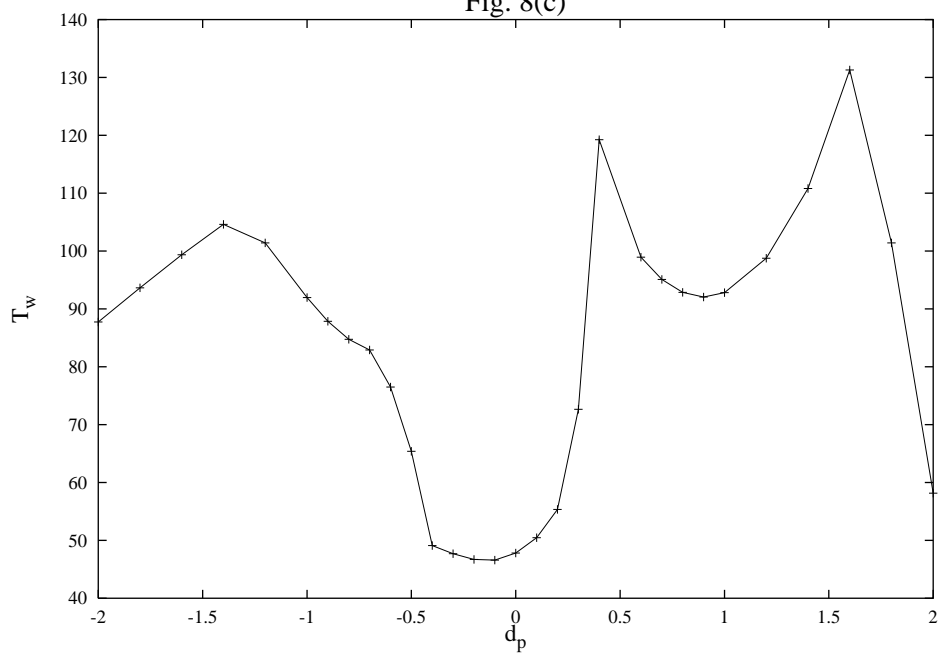


Fig. 8: Geometry of the two particle system used for the analytical estimate of T_w . A particle (shaded) is fixed at $(0, 0)$, and a mobile particle starts d away from it, in the ambient velocity field $U^\infty = (\cos \theta, \sin \theta, 0)$.

Fig. 9(a)

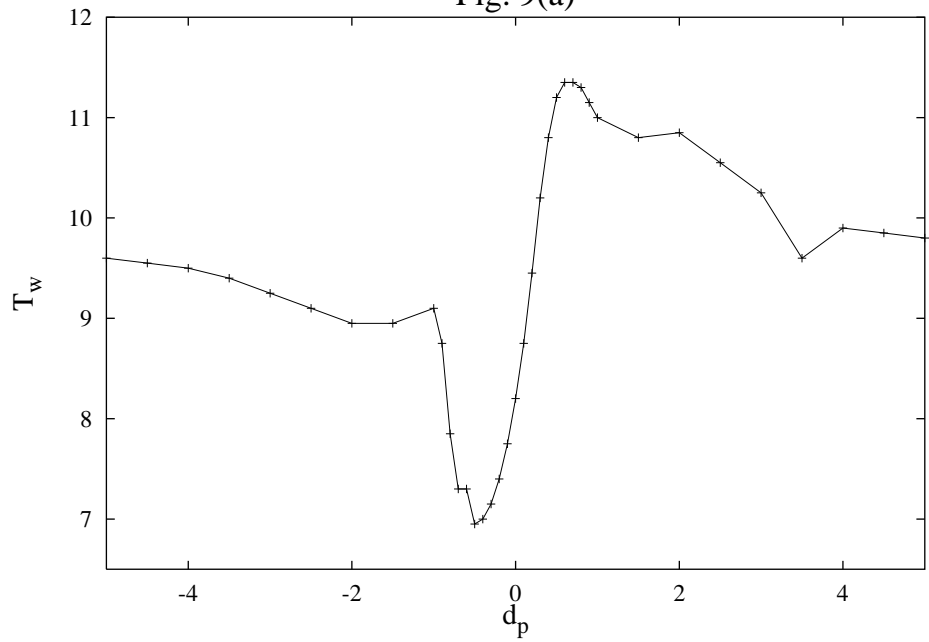


Fig. 9(b)

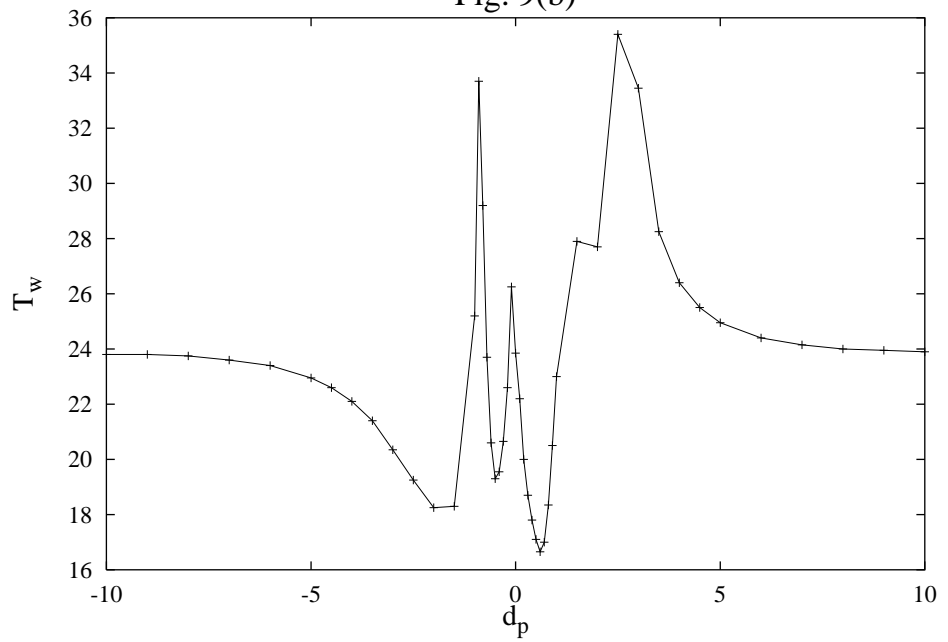


Fig. 9(c)

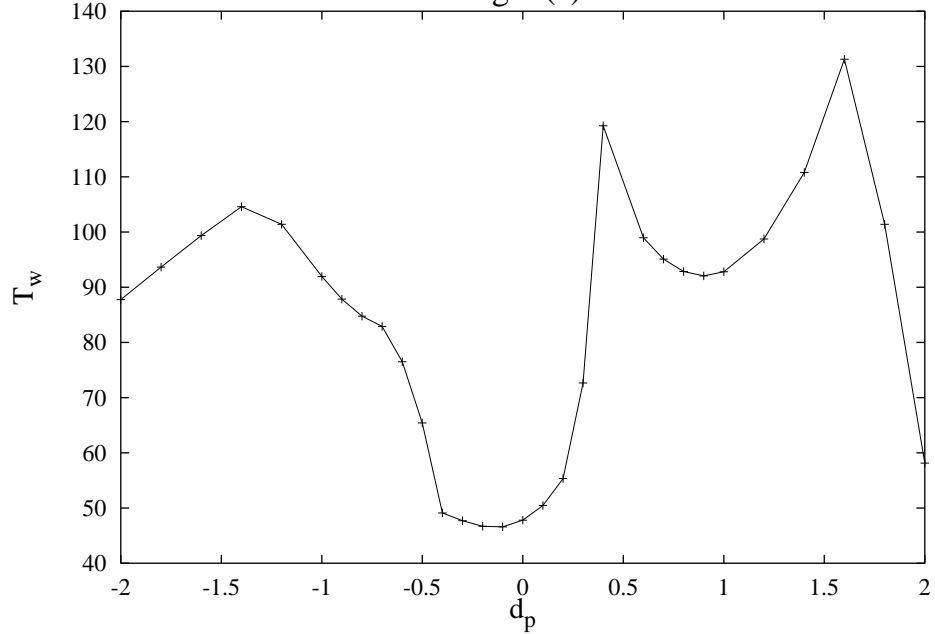


Fig. 9: Waiting time distributions for the perturbation of a slow particle. A mobile particle is at $(-2.2, d_w, 0)$ in front of a fixed particle, while a second mobile particle starting at $(-5, d_p, 0)$ passes by. The waiting time for the first particle is plotted against d_p for (a) $d_w = 0.1$, and (b) $d_w = 0.01$. (c) The waiting time for a mobile particle in the 2d-11 geometry, in the presence of another mobile particle. The variable d_p is roughly the impact parameter of the second mobile particle.

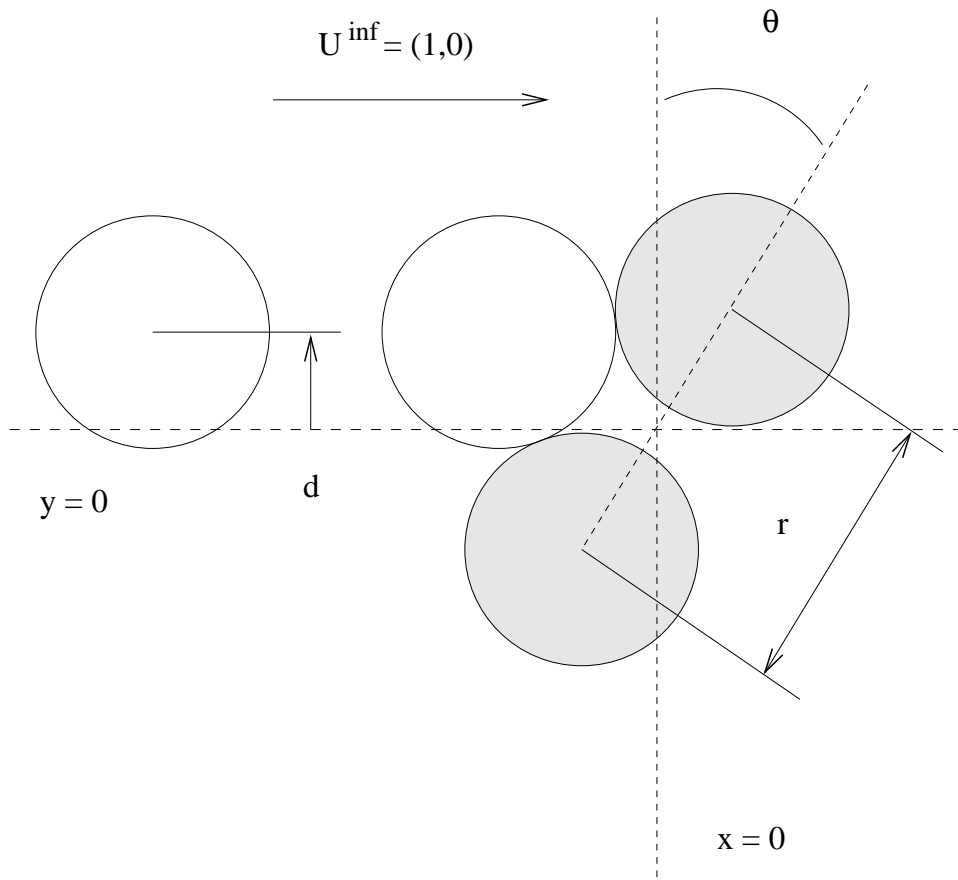


Fig. 10

Fig. 10: Geometry for studying the relaunching of trapped particles. A mobile particle is in a model two-particle trap (marked with grey shade) characterized by r and θ , while another mobile particle starting at $(-5, d, 0)$ passes near the trap.

Fig. 11

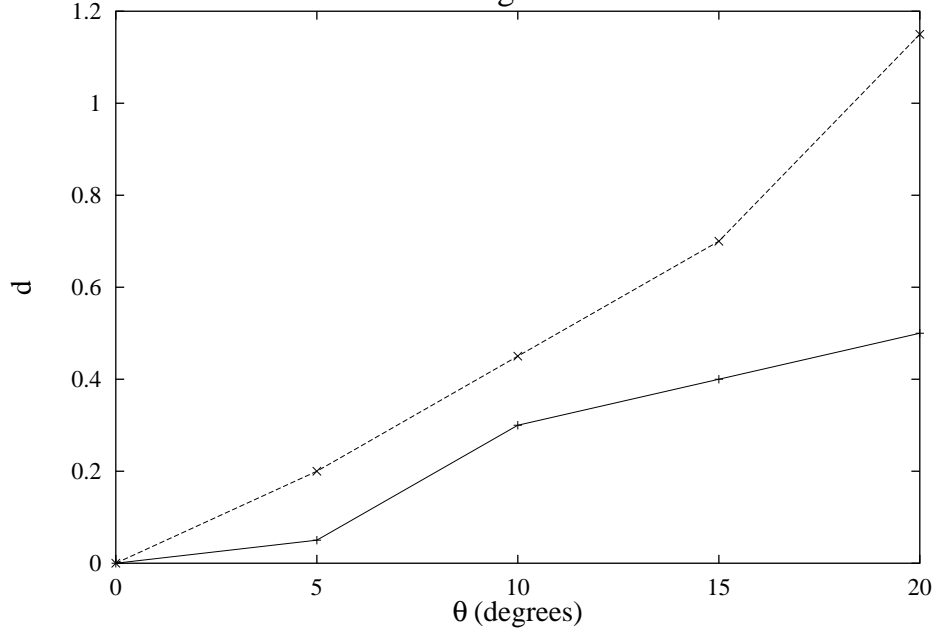


Fig. 11: The range of d for which relaunching occurs plotted against θ , for the geometry in Fig. 10 with $r = 2$. The relaunching occurs in the region bounded by the two lines.